ELSEVIER

Materials Science and Engineering A 438–440 (2006) 288–291

MATERIALS SCIENCE & ENGINEERING A

www.elsevier.com/locate/msea

Analytical transmission electron microscopy study of grain boundary precipitates in an Fe–Ni–Mn maraging alloy

S. Hossein Nedjad [a,*], M. Nili Ahmadabadi [b], R. Mahmudi [b], T. Furuhara [c], T. Maki [d]

[a] *Faculty of Materials Engineering, Sahand University of Technology, P.O. Box 51335-1996, Tabriz, Iran*
[b] *School of Metallurgy and Materials Engineering, Faculty of Engineering, University of Tehran, P.O. Box 14395-731, Tehran, Iran*
[c] *Institute for Materials Research, Tohoku University, 2-1-1 Katahira, Aoba-ku, Sendai 980-8577, Japan*
[d] *Department of Materials Science and Engineering, Kyoto University, Yoshida-Honmachi, Sakyo-ku, Kyoto 606-8501, Japan*

Received 13 June 2005; received in revised form 6 February 2006; accepted 28 February 2006

Abstract

Field-emission gun analytical transmission electron microscopy was used to study grain boundary precipitates in Fe–10Ni–7Mn (wt.%) maraging alloy after isothermal aging at 753 K. High spatial resolution energy dispersive X-ray spectroscopy was used for quantitative chemical analysis of the grain boundary precipitates. Precipitation of f.c.t. θ-NiMn intermetallic compound and reversion to f.c.c. austenite were identified at prior austenite grain boundaries after prolonged aging. Selected area electron diffraction patterns (SADPs) showed the $L1_0$ type ordering of f.c.t. θ-NiMn precipitates. The f.c.t. θ-NiMn precipitates showed higher Ni and Mn concentrations than reverted f.c.c. austenite.

Keywords: Maraging; Grain boundary; Precipitation; Reverted austenite; NiMn

1. Introduction

Fe–Ni–Mn maraging alloys have attracted increasing interest because of their economic aspects. Successive precipitation of f.c.t. θ-NiMn intermetallic compound and reversion to f.c.c. austenite has been found in these alloys during isothermal aging. The typical age hardening and softening phenomena during isothermal aging have been attributed to precipitation of f.c.t. θ-NiMn and reversion to f.c.c. austenite, respectively [1].

Fe–Ni–Mn maraging alloys are sufficiently ductile in the solution annealed condition but suffer from severe intergranular embrittlement along prior austenite grain boundaries (PAGBs) after aging [2,3]. The source of grain boundary embrittlement in these alloys has been attributed to grain boundary segregation and precipitation. For example, segregation of Mn atoms at PAGBs has been proposed to take place during isothermal aging [2,4]. Mun et al. [5] reported precipitation of f.c.c. reverted austenite particles at PAGBs in Fe–8Mn–7Ni (wt.%) alloy. Lee et al. [6] reported precipitation of f.c.t. θ-NiMn intermetallic compound at PAGBs in Fe–10Ni–5Mn (wt.%) alloy. Hossein Nedjad et al. [7] found discontinuous coarsening of f.c.t. θ-NiMn intermetallic precipitates at PAGBs during isothermal aging of Fe–10Ni–7Mn (wt.%) alloy at 753 K.

Recent studies have explored the role of grain boundary precipitates in premature intergranular failure of Fe–Ni–Mn maraging alloys where identification of grain boundary precipitates and mechanism of grain boundary failure remain controversial yet [5–7]. For instance, f.c.c. austenite has been reported as responsible for grain boundary failure [5] while reversion to austenite has been reported frequently to increase ductility at later stages of aging in Fe–Ni–Mn maraging alloys [2,6,7]. The θ-NiMn intermetallic compound has a face centered tetragonal (f.c.t.) crystal structure ($a = 0.372$ nm, $c = 0.353$ nm and $c/a = 0.95$) which is almost identical to the face centered cubic (f.c.c.) crystal structure of the reverted austenite ($a = 0.358$ nm) [5]. Consequently, selected area electron diffraction (SAD) techniques would show some difficulty to identify these phases due to their similar crystal structure. Meanwhile, chemical analysis of these precipitates can be proposed as supplementary method for phase identification.

The aim of this paper is to study grain boundary precipitates in Fe–10Ni–7Mn (wt.%) maraging alloy by analytical transmission electron microscopy.

* Corresponding author. Tel.: +98 412 345 80 33; fax: +98 412 344 43 33.
E-mail address: hossein@sut.ac.ir (S. Hossein Nedjad).

0921-5093/$ – see front matter © 2006 Elsevier B.V. All rights reserved.
doi:10.1016/j.msea.2006.02.097

Table 1
Chemical composition of the alloy studied (wt.%)

Fe	Base
Ni	10.38
Mn	6.88
C	0.006
S	0.007
P	0.005
N	0.005
Al	0.003

2. Experimental procedure

A vacuum induction melted and vacuum arc remelted material was encapsulated in a quartz tube and argon gas was purged after evacuation to 10^{-5} Torr. Chemical composition of the prepared alloy is given in Table 1. A homogenizing treatment was performed at 1473 K for 172.8 ks followed by water quenching. Cold rolling to 85% reduction was carried out at room temperature before solution annealing treatment at 1223 K for 3.6 ks in a vacuum furnace followed by water quenching and subzero treatment at 77 K for 3.6 ks. Isothermal aging treatment was carried out at 753 K in a neutralized salt bath.

Disc-shaped specimens (diameter 3 mm; initial thickness 300 μm) were cut using an electro discharge wire cutting machine and then mechanically polished to a thickness of ca. 30 μm. Further thinning was accomplished electrochemically in a solution of CrO_3 (200 g), CH_3COOH (500 ml) and H_2O (40 ml) held at 285 K and using a voltage of 22–25 V by a twin jet Struers TENOPUL-3 electropolishing machine. Transmission electron microscopy studies were carried out with PHILIPS CM200-FEG microscope operating at 200 kV. Chemical compositions of phase constituents were measured using high spatial resolution energy dispersive X-ray spectroscopy (EDS) microanalysis with a nominal beam diameter of 1.8 nm using EDAX detector assembled on the CM200-FEG microscope.

Thermodynamic calculations of chemical compositions were performed by Thermocalc (Version P) using Kaufman binary alloys database.

3. Results and discussion

Fig. 1 shows age hardening curve of the Fe–10Ni–7Mn (wt.%) alloy during isothermal aging at 753 K indicating a typical maraging behavior of this alloy. Fig. 2a shows a bright field TEM image of grain boundary precipitates in a specimen aged for 86.4 ks. Arrows indicate coarse precipitates where some of them have been embedded in a precipitate free zone lying at lower side of the grain boundary. Fig. 2b shows selected area electron diffraction pattern (SADP) obtained from these grain boundary precipitates indicating them as f.c.t. θ-NiMn intermetallic compound. This configuration of grain boundary precipitation is attributed to discontinuous coarsening of f.c.t. θ-NiMn precipitates and will be published in detail elsewhere. Fig. 3a shows a bright field TEM image of large particles

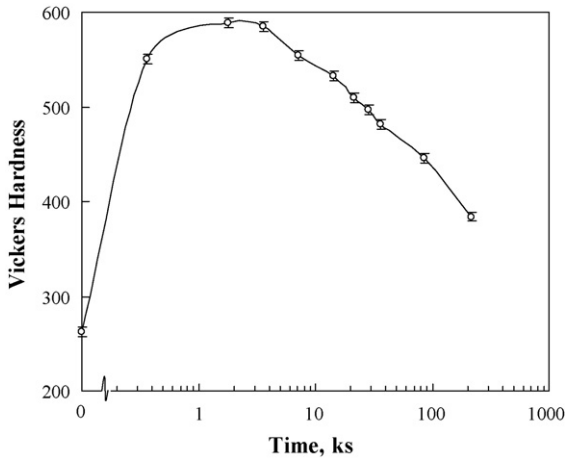

Fig. 1. Age hardening behavior of the studied alloy during isothermal aging at 753 K.

(arrows) at a PAGB in a specimen aged for 86.4 ks. SADP obtained from these particles is shown in Fig. 3b indicating them as f.c.c. reverted austenite holding a near Kurdjamov-Sachs type orientation relationship with b.c.c. iron matrix. SADPs of an f.c.c. austenite and an f.c.t. θ-NiMn precipi-

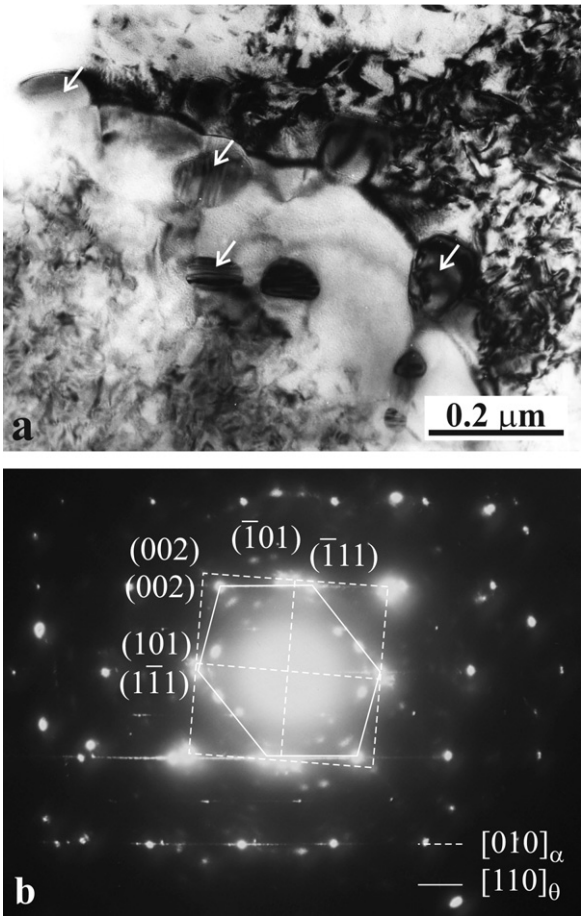

Fig. 2. Bright field TEM image showing coarse f.c.t. θ-NiMn precipitates (arrows) at a PAGB in a specimen aged for 86.4 ks; (b) SADP obtained from the grain boundary precipitates.

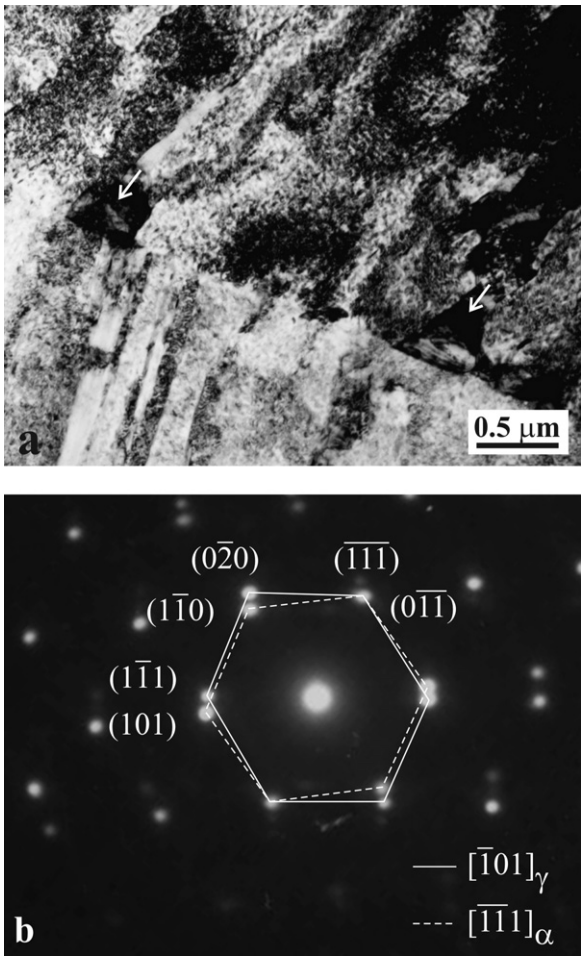

Fig. 3. (a) Bright field TEM image showing reverted austenite particles (arrows) at a PAGB in a specimen aged for 86.4 ks; (b) SADP obtained from the reverted austenite particles.

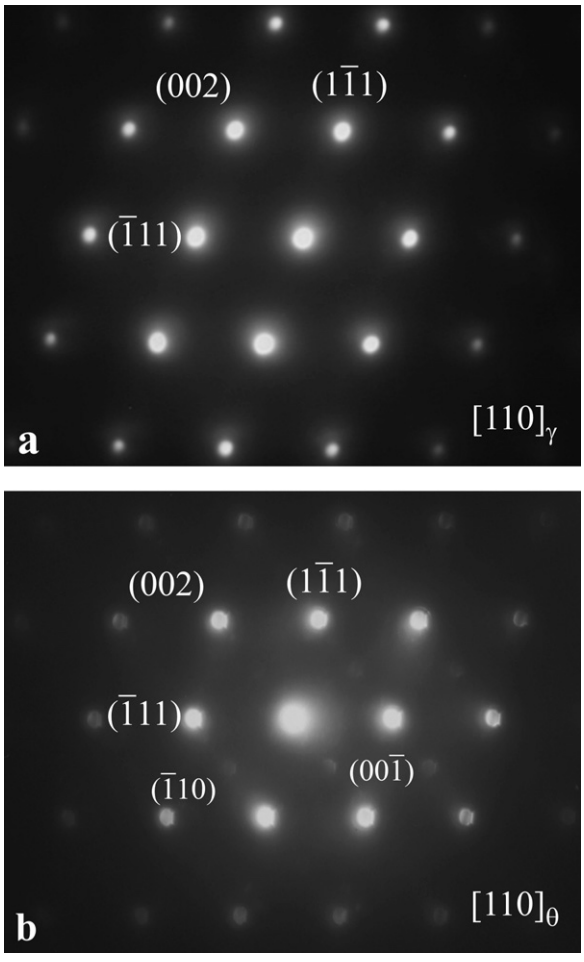

Fig. 4. SADPs of grain boundary phases in a specimen aged for 86.4 ks: (a) f.c.c. reverted austenite; (b) f.c.t. θ-NiMn. Note superlattice spots in (b) corresponding to (0 0 $\bar{1}$) and ($\bar{1}$ 1 0).

tate are shown in Fig. 4a and b, respectively, corresponding to the [1 1 0] zone axes for both phases. There are superlattice spots corresponding to (0 0 $\bar{1}$) and ($\bar{1}$ 1 0) planes in Fig. 4b which indicate the $L1_0$ (CuAu I type) ordering of f.c.t. θ-NiMn precipitate.

Fig. 5a and b show EDS spectra obtained from f.c.c. reverted austenite and f.c.t. θ-NiMn, respectively, in a specimen aged for 86.4 ks. Typical quantitatively measured chemical compositions of f.c.c. reverted austenite and f.c.t. θ-NiMn intermetallic compound are shown in Table 2. Calculated chemical composition of f.c.c. phase by Thermocalc and stoichiometric composition of NiMn phase are also shown inside parenthesis in Table 2. The experimental, calculated and stoichiometric chemical compositions indicate an obvious difference between f.c.c. reverted austenite and f.c.t. θ-NiMn phases, i.e. lower Ni and Mn concentrations in the f.c.c. reverted austenite. However, there is a large difference between the calculations and measurements. Interferences between electron beams and surrounding matrices, resulting in iron pick-up from the matrices, might confuse the measured values. Austenite laths with chemical composition similar to the nominal composition (83Fe–10Ni–7Mn (wt.%)) was found frequently in the specimen aged for 86.4 ks. T_0 was calculated for this alloy of about 679 K which indicates possibility of non-reconstructive transformation mechanism where austenite retention can also be assumed. Mun et al. [5] reported chemical compositions of grain boundary precipitates in Fe–8Mn–7Ni (wt.%) alloy in the range of 15–30 wt.% Ni and 15–30 wt.% Mn. Lee et al. [6] measured chemical composition of grain boundary f.c.t. θ-NiMn precipitates in Fe–10Ni–5Mn (wt.%) alloy close to 51.7Ni–48.3Mn (wt.%). Thermodynamic calculations indicated that chemical composition of f.c.c. reverted austenite depends strongly on the alloy composition showing Ni to Mn ratio close to nominal composition while an stoichiometric composition of 51.7Ni–48.3Mn (wt.%) can be proposed for f.c.t. θ-NiMn precipitates [7].

Table 2
Chemical compositions of f.c.c. reverted austenite and f.c.t. θ-NiMn phases (wt.%)

Phase	Fe	Ni	Mn
f.c.c. austenite	71.5 (51.8[a])	16.0 (28.9[a])	12.5 (19.4[a])
f.c.t. θ-NiMn	20.5 (0.0[b])	43.4 (51.7[b])	36.1 (48.3[b])

[a] Calculated by Thermocalc.
[b] Stoichiometric chemical composition.

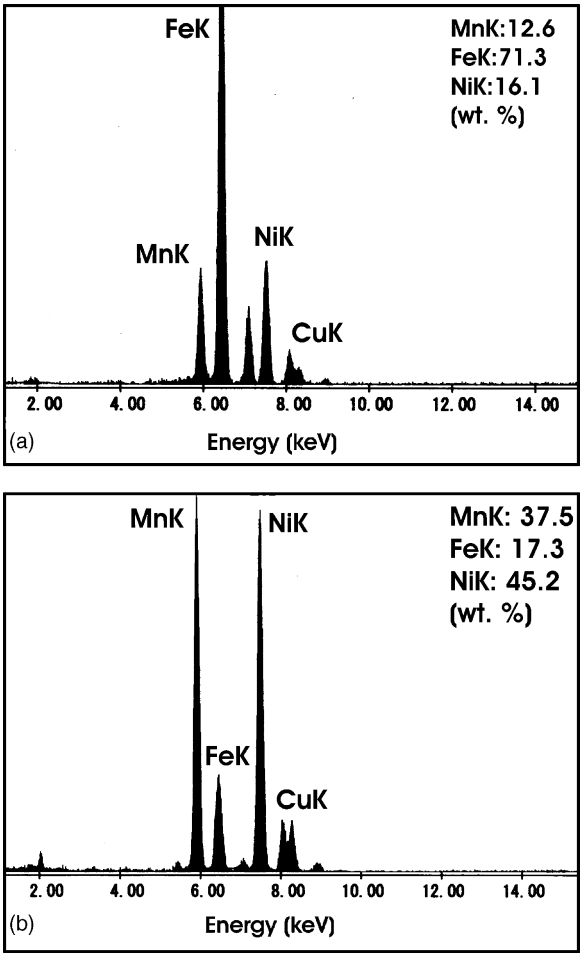

Fig. 5. Typical EDS microanalysis spectra of grain boundary phases in a specimen aged for 86.4 ks: (a) f.c.c. reverted austenite; (b) f.c.t. θ-NiMn. Values on the spectra indicate quantitative analysis.

Mun et al. [5] and Lee et al. [6] have identified grain boundary precipitates as f.c.c. austenite and f.c.t. θ-NiMn precipitate in Fe–8Mn–7Ni (wt.%) and Fe–10Ni–5Mn (wt.%) maraging alloys, respectively. Precipitation of f.c.t. θ-NiMn intermetallic compound and f.c.c. reverted austenite at PAGBs were confirmed in the present Fe–10Ni–7Mn (wt.%) maraging alloy by EDS microanalysis and SADPs.

4. Conclusions

1. Typical chemical compositions of f.c.t. θ-NiMn and f.c.c. reverted austenite in Fe–10Ni–7Mn (wt.%) maraging alloy were measured as 20.5Fe–43.4Ni–36.1Mn (wt.%) and 71.5Fe–16.0Ni–12.5Mn (wt.%) by EDS microanalysis, respectively.
2. Precipitation of f.c.t. θ-NiMn intermetallic compound at PAGBs was confirmed using high spatial resolution EDS microanalysis and SADPs. Reversion to f.c.c. austenite was also identified at later stages of aging.

References

[1] M. Yodogawa, Trans. JIM 17 (1976) 799–808.
[2] D.R. Squires, E.A. Wilson, Metall. Trans. 3 (1972) 575–581.
[3] S. Hossein Nedjad, M. Nili Ahmadabadi, R. Mahmudi, H. Farhangi, Mater. Sci. Eng. A738 (2004) 314–318.
[4] N.M. Heo, Metall. Mater. Trans. 27A (1996) 1015–1020.
[5] S.H. Mun, M. Watanabe, X. Li, K.H. OH, D.B. Williams, H.C. Lee, Metall. Mater. Trans. 33A (2002) 1057–1067.
[6] H.C. Lee, S.H. Mun, D. McKenzie, Metall. Mater. Trans. 34A (2003) 2421–2428.
[7] S. Hossein Nedjad, PhD thesis, University of Tehran, 2005.